$Fe(CN)_6^{3-}$ are no longer confined to a small part of the system which encourages rapid reaction, but are now spread throughout larger structures. The reaction rate drops and the lifetimes of (RuII)* increases.

It is noteworthy that the polarization of diphenylhexatriene decreases abruptly at 40% water when the large structures start to be formed. This probe is located in the oil part of the system and indicates a disruption of the oil as the larger structures are formed leading to a higher mobility of the probe. At larger water contents the polarization increases again as the system forms a more organized assembly.

Reaction rate constants given in Table II for several pyrene chromophores and quenchers indicate the compartmentalized nature of the system. The probes PBA and PSA and quenchers Tl^+ and I^- are located in the water pools. Tl^+ is probably in the vicinity of the head-group region near the carboxylate groups, while I^- is repelled into the pool. Pyrene is located only in the alkane, but may approach the pool, while DMA and O_2 move fairly freely through the system. The quenching rate constants of DMA and O_2 with pyrene, PSA, and PBA are similar in keeping with the model given above. Iodide ion quenches both PSA and PBA, but not pyrene as this probe cannot enter the water pool interior. Thallous ion quenches all three probes but pyrene least efficiently, although this is more efficient than the case of I^-. This is in keeping with Tl^+ being located at the interface and an inefficient approach of pyrene to this region of the system.

If a k of 10^{10} L M^{-1} s^{-1} is assumed for O_2 reacting with the probes, then the $[O_2]$ can be calculated in the bulk hydrocarbon, and in the water pool. The $[O_2]$ is larger in the hydrocarbon than in the water, again in keeping with the established solubilities of O_2 in the bulk liquids.

These studies establish the kinetic patterns that take place with photoinduced reactions in oleate microemulsions. The kinetics follow structural changes in the system, which are also monitored by other physical measurements. These data are useful in designing micellar systems that act as models for biological membranes, and for solar energy research. In particular the compartmentalized nature of the systems leads to rapid reaction of excited species. The subsequent fate of the products, which are often ionic, depends on the exit rate one pool to another, and on the nature of the assembly produced under the existing matrix composition.

Electronic Structure of the Phosphenium Ions PH_2^+, HPF^+, and PF_2^+ §

James F. Harrison[1]

Contribution from the Theoretical Chemistry Group, Chemistry Division, Argonne National Laboratory, Argonne, Illinois 60439. *Received March 20, 1981*

Abstract: The geometry, total energy, and charge distribution of the three lowest states of the divalent phosphorus cations PH_2^+, HPF^+, and PF_2^+ are reported using ab initio generalized valence bond (GVB) wave functions and for PH_2^+ configuration interaction wave functions. The character of the valence orbitals is analyzed and related to the nature of the PH and PF bonds in the $^2\pi$ and $^4\Sigma^-$ states of PH^+ and PF^+. GVB calculations predict that each molecule has a singlet ground state with the next electronic state being a triplet, some 20.4, 42.6, and 84.0 kcal/mol higher for PH_2^+, HPF^+, and PF_2^+, respectively. CI calculations on PH_2^+ reduce this singlet–triplet separation to 16.4 kcal/mol.

In the past few years reactions of Lewis acids with various amino halophosphines have resulted in solutions,[2] transition-metal complexes,[3] and most recently isolable phosphenium salts.[4,5] These latter substances (such as the bis(dialkylamino)phosphenium ion $[(CH_3)_2NPN(CH_3)_2]^+$) have well defined NMR spectra and are presumed to be electronically ground state singlets. Phosphenium ions are also present in the mass spectra[6] of numerous phosphorus compounds but are not at all structurally well defined. That the multiplicity should be in question at all is easily seen by noting that the phosphenium ions are isovalent with nitrenium ions, carbenes, and silylenes, all of which count singlets and triplets among their members. As a first step in understanding the structure of these molecules we have studied the parent ion PH_2^+ as well as the mono- and difluoro compounds PHF^+ and PF_2^+. Specifically we have determined, for each molecule, the singlet–triplet separation, the lowest singlet–singlet separation, and to the extent presently possible, the charge distribution. In addition to providing insight into the structure of an increasingly important class of molecules these results will improve our understanding of substituent effects in the isovalent carbenes, nitrenium ions, and silylenes.[7]

Technical Details

A. Basis Sets. The basis functions are characterized in Table I. The primitive sets are from Huzinaga[8] and have been contracted as recommended by Raffenetti.[9] The exponents of the hydrogen s functions were scaled by 1.2 and each atom was endowed with a set of single component polarization functions. The phosphorus d and hydrogen p exponents were optimized in the lowest singlet state of PH_2^+ while the fluorine d exponent was taken as recommended by Dunning and Hay.[10] The number of contracted functions used for each molecule is 29 (PH_2^+), 39 (PHF^+), and 49 (PF_2^+).

Table I. Basis Set

atom	primitive basis	contraction	polarization function	total contracted
P	11s,7p	4s,3p	1d ($\alpha = 0.5$)	19(4s,3p,1d)
F	9s,5p	3s,2p	1d ($\alpha = 0.9$)	15(3s,2p,1d)
H	4s	2s	1p ($\alpha = 0.6$)	5(2s,1p)

§ Work performed under the auspices of the Office of Basic Energy Sciences, Division of Chemical Sciences, U.S. Department of Energy.

(1) Scientist in Residence, Argonne National Laboratory 1980/81. Address correspondence to the following address: Department of Chemistry, Michigan State University, East Lansing, MI 48824.

(2) S. Fleming, M. K. Lupton, and K. Jekot, *Inorg. Chem.*, **11**, 2534 (1972).

(3) (a) R. W. Light and R. T. Paine, *J. Am. Chem. Soc.*, **100**, 2230 (1978). (b) R. G. Montemayor, D. T. Sauer, S. Fleming, D. W. Bennelet, M. G. Thomas, and R. W. Parry, *ibid.*, 2231 (1978).

(4) A. H. Cowley, M. C. Cushmer, and J. S. Szobota, *J. Am. Chem. Soc.*, **100**, 7784 (1978).

(5) L. D. Hutchins, R. T. Paine, and C. F. Compana, *J. Am. Chem. Soc.*, **102**, 4521 (1980).

(6) M. Halmann, *J. Chem. Soc.*, 3270 (1962). Also, see the review by I. Granoth in "Topics in Phosphorous Chemistry", Vol. 8, E. J. Griffith and M. Grayson, Eds., Wiley, New York, 1976.

(7) J. F. Harrison, R. C. Liedtke, and J. F. Liebman, *J. Am. Chem. Soc.*, **101**, 7162 (1979), and references contained within.

(8) S. Huzinaga, *J. Chem. Phys.*, **42**, 1293 (1965); Approximate Atomic Wave Functions, I & II, Technical Report from the Theoretical Chemistry Division, University of Alberta, Edmonton, Alberta 1971.

(9) R. C. Raffenetti, *J. Chem. Phys.*, **58**, 4452 (1973).

(10) T. H. Dunning, Jr., and P. J. Hay, "Modern Theoretical Chemistry", Vol. 2, H. F. Schaefer III, Ed., Plenum, New York, 1976.

0002-7863/81/1503-7406$01.25/0

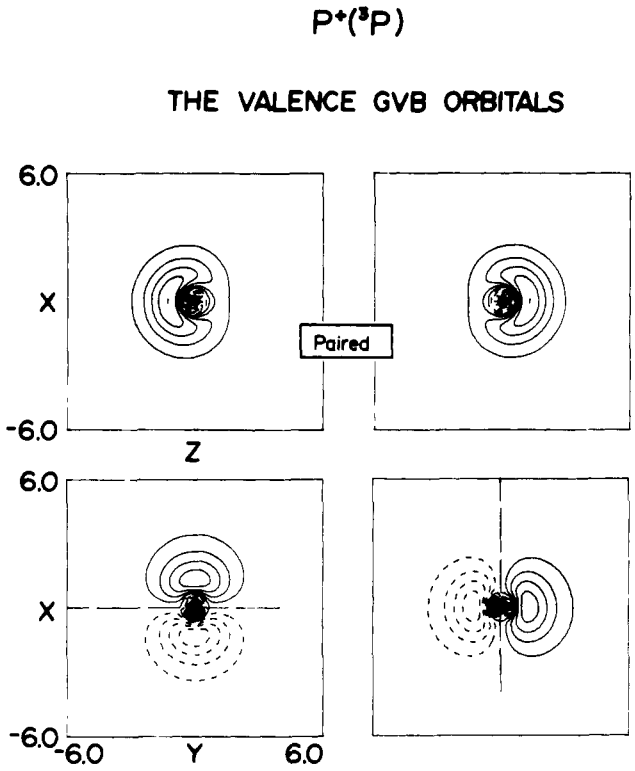

Figure 1. The GVB valence orbitals l_z, $l_{\bar{z}}$, p_x, and p_y for the ^3P state of P^+. The plots have uniformly spaced contours with increments of 0.05 au. Positive contours are indicated by solid lines, negative contours are indicated by dotted lines, and nodal planes are indicated by long dashes. The same conventions are used for all plots.

B. Molecular Codes. The calculations reported in this paper were carried out at Argonne National Laboratory using the system of codes indicated below.

The integral evaluation and transformations were carried out with the programs BIGGMOLI[9] and TRAOMO written by R. C. Raffenetti. The GVB wave functions were constructed with the program GVBTWO, originally written by F. Bobrowicz and W. Wadt with latter modifications by L. G. Yaffe, A. K. Rappe, and others. The configuration lists for the CI calculations were generated by the program GENCFG written by R. C. Lander and B. D. Olafson with modifications by S. P. Walch and T. H. Dunning, Jr. The CI calculations were carried out using the program CITWO written by F. W. Bobrowicz with extensive modifications by S. P. Walch. The contour plots were generated using a version of the Cal Tech program CONTURM as modified by S. P. Walch and R. C. Raffenetti to make use of the general contraction scheme.

The Fragments

A. The Atoms. Although the focus in this study is not on how the various phosphenium ions might be formed from the possible fragments, it is instructive to consider the stepwise formation from the separated atoms. Since the ionization potential of phosphorus is 11.00 eV, while hydrogen and fluorine are 13.60 and 17.42 eV, respectively, we will consider the separated atoms to be P^+ F, and H.

In the Hartree–Fock description of this ^3P state of P^+ the electronic configuration is

$$1s^2 2s^2 2p^6 3s^2 3p^2$$

where the two electrons in the 3p orbital are triplet coupled. In the generalized valence bond[11] description of this atom each electron is assigned to a different spatial orbital so, for example, the two electrons which, in the Hartree–Fock model, both occupy the 1s orbital of phosphorus would occupy different orbitals, say $1s_a$ and $1s_b$ where $\langle 1s_a|1s_b\rangle \neq 0$. It happens that for these two orbitals the overlap is essentially 1 and the difference between 1s, $1s_a$, and $1s_b$ is so slight as to be unimportant in describing the atom, and the HF and GVB descriptions of the inner shell 1s pair are essentially identical. The same equivalence obtains for the 2s, 2p, and 3p orbitals of P^+ but not for the 3s. If the occupied 3p orbitals in P^+ are $3p_x$ and $3p_y$ the GVB orbitals which replace the HF 3s orbitals are of the form

$$(3s \pm \lambda\, 3p_z)(1 + \lambda^2)^{-1/2}$$

where $\lambda = 0.36$. These GVB orbitals for the valence shell of P^+ are shown in Figure 1. The two GVB orbitals which replace the single HF 3s orbital are called lobe orbitals and as is evident from Figure 1 they have considerable directional character. Suppressing all but the valence electrons we may write the GVB function for the ^3P state of P^+ as

$$\mathcal{A}(\text{core})l_z l_{\bar{z}}(\alpha\beta - \beta\alpha)p_x p_y \alpha\alpha$$

with the schematic representation

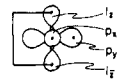

where the p orbitals parallel and perpendicular to the plane are represented by

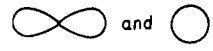

and the GVB lobe orbitals by

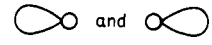

The line connecting the lobes represents a singlet coupling of the associated electrons. The HF and GVB orbitals of F are essentially identical and we will not attempt to distinguish between them. Our schematic representation of $F(^2P)$ is

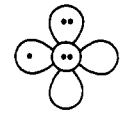

The atomic energies as calculated with our basis are collected in Table II.

Table II. Fragment Energies

species	state	R, bohr	energy, hartrees	bond energy, kcal/mol
P^+	^3P		−340.334712	
F	^2P		−99.396923	
H	^2S		−0.49928	
$(PH)^+$	$^2\pi$	2.715	−340.94039	−66.8
$(PH)^+$	$^4\Sigma^-$	2.705	−340.88054	−29.2
$(PF)^+$	$^2\pi$	2.871	−439.86552	−84.0
$(PF)^+$	$^4\Sigma^-$	2.915	−439.72039	+7.1

B. The Diatomics. When a hydrogen atom (represented by ⊙) approaches the P^+ ion (^3P state) it may do so along a singly occupied p orbital direction (forming a bond to the p orbital)

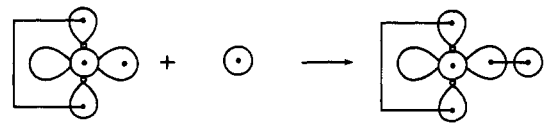

resulting in a $^2\pi$ state. Alternatively it may approach along one of the lobe directions

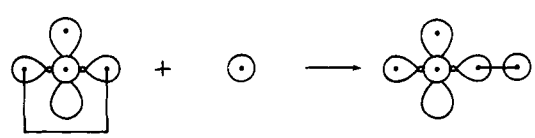

(11) W. A. Goddard III, T. H. Dunning, Jr., W. J. Hunt, and P. J. Hay, *Acc. Chem. Res.*, **6**, 368 (1973).

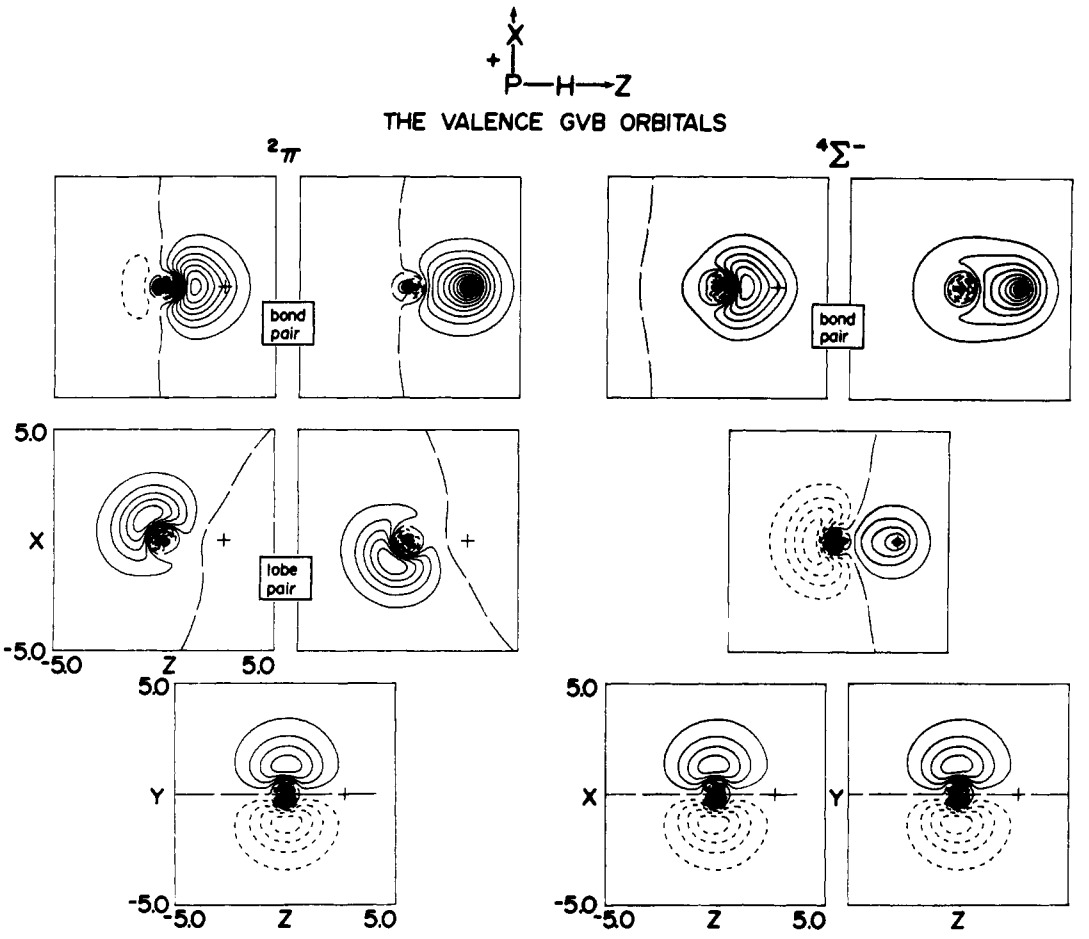

Figure 2. The GVB valence orbitals for PH^+ in the $^2\pi$ and $^4\Sigma^-$ states.

resulting in a $^4\Sigma^-$ state.

Fluorine of course has the same options. The singly occupied F p orbital could bond to the single occupied P^+ orbital, resulting in a $^2\pi$ state

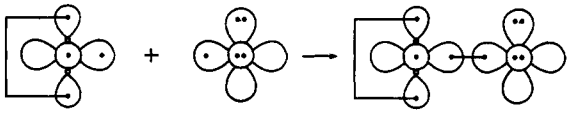

or it could bond to a lobe orbital on P^+ resulting in a $^4\Sigma^-$ state

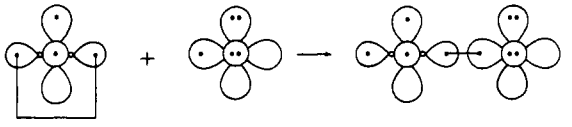

The relative merits of bonding to a p orbital or to a lobe have been discussed in the literature and the excellent review articles by Goddard[11] et al. and Goddard and Harding[12] should be consulted for details.

The wave functions for the $^2\pi$ states of $(PH)^+$ and $(PF)^+$ were constructed with all but 5 electrons assigned to doubly occupied, HF-like, spatial orbitals. These 5 electrons were each assigned to individual spatial orbitals as follows: two were singlet coupled to form the bond, two were singlet coupled and represent the lobe orbitals, and the last was assigned to the open shell π orbital.

The wave functions for the $^4\Sigma^-$ states also have all but 5 electrons assigned to doubly occupied spatial orbitals. These 5 electrons are allotted to individual orbitals and three (one of π_x, one of π_y, and one of σ symmetry) are coupled into a quartet spin symmetry while two of σ symmetry are singlet coupled and represent the bond. All orbitals are solved for self-consistently. The calculated bond lengths, total energy, and bond energies are collected in Table II and contour maps of the valence orbitals are shown in Figures 2 and 3.

Note that for both PH^+ and PF^+ the calculations predict $^2\pi$ ground states in agreement with experiment.[13] In addition the calculated bond lengths (2.715 bohr for PH^+ and 2.871 bohr for PF^+) are in reasonable agreement with the experimental values[13] (2.693 bohrs for PH^+ and 2.835 bohrs for PF^+). Further, while the $^4\Sigma^-$ state of PH^+ is bound by (at least) 29.2 kcal/mol, the corresponding state of PF^+ is calculated to be unbound relative to the separated atoms. While the question of whether $(PF)^+$ is bound in the $^4\Sigma^-$ state is interesting it is not one we will pursue. Instead we will interpret our results on these diatomics as demonstrating that when a hydrogen or fluorine atom bonds to a P^+ ion the most favorable interaction, by far, is with the singly occupied p orbital on P^+. This is consistent with previous studies[11] on CH and CF where the $^2\pi$ was also the ground state with the $^4\Sigma^-$ being 17 and 64 kcal/mol higher in each case. Note that the $^2\pi - {}^4\Sigma^-$ separation increases along the series CH, PH^+, CF, and PF^+.

The contour plots of the P–H bonding orbitals (Figure 2) suggest that in both the $^2\pi$ and $^4\Sigma^-$ states the P–H bond is covalent, i.e., one orbital centered on P and the other on H. They also confirm the anticipated difference in the bond character in the $^2\pi$ and $^4\Sigma^-$ states. In the $^2\pi$ state the P-centered bond orbital has significant p character (note the node containing the P nucleus) while in the $^4\Sigma^-$ state the corresponding bond orbital is much more lobe-like (note the absence of an angular node containing the P nucleus). Also, while the singlet coupled lobes in the $^2\pi$ state are still localized on phosphorus they no longer make an angle of 90° with the internuclear line. Instead they are bent back by the

(12) W. A. Goddard III and Lawrence B. Harding, *Annu. Rev. Phys. Chem.*, **29**, 363 (1978).

(13) N. A. Narasimhan, *Can. J. Phys.*, **35**, 901 (1957), and A. E. Douglas and M. Franckowiak, *Can. J. Phys.*, **40**, 832 (1962).

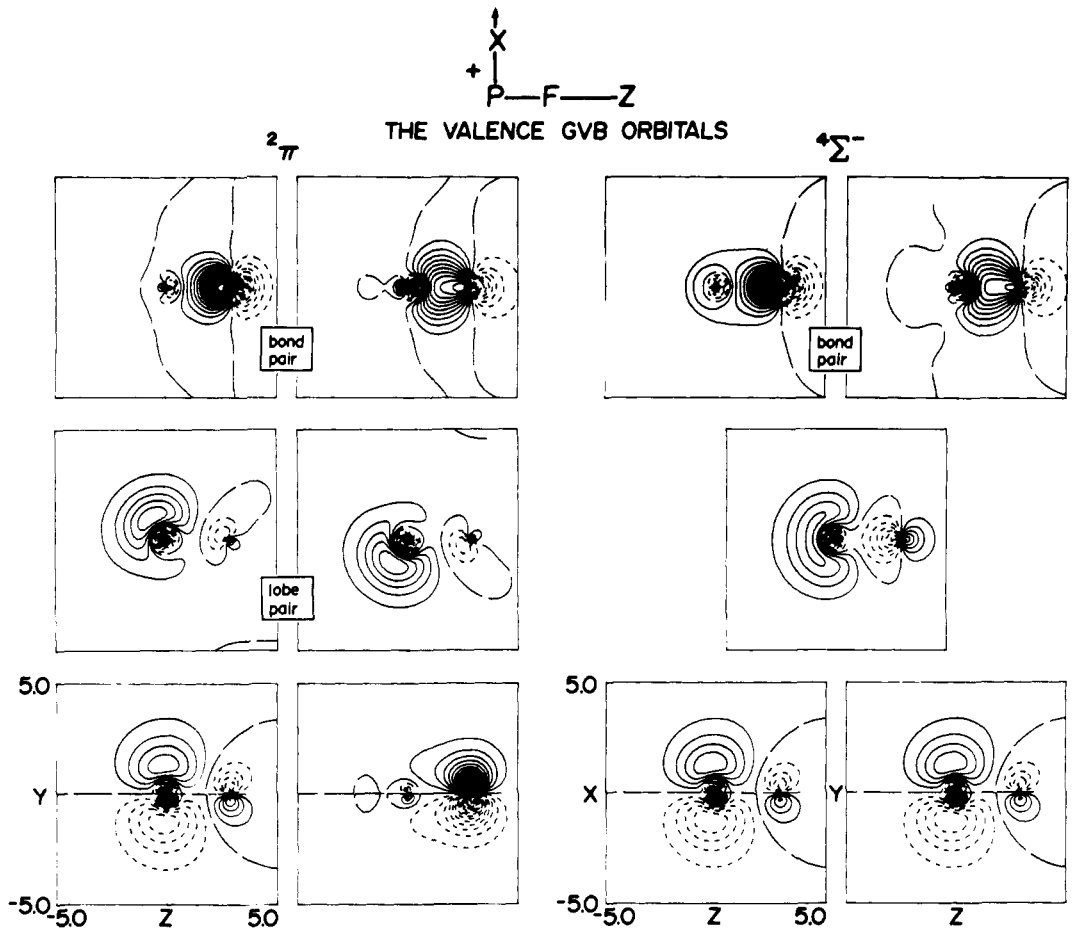

Figure 3. The GVB valence orbitals for PF^+ in the $^2\pi$ and $^4\Sigma^-$ states.

Table III. GVB Calculations of Energy and Geometry of PH_2^+, HPF^+, and PF_2^+

molecule	state	R(P-H), bohr	R(P-F), bohr	θ, deg	energy, hartrees
PH_2^+	$^1A_1$	2.714		94.0	−341.562170
PH_2^+	$^3B_1$	2.667		121.5	−341.529685
PH_2^+	$^1B_1$	2.679		126.6	−341.466201
HPF^+	$^1A'$	2.876	2.876	95.0	−440.481499
HPF^+	$^3A''$	2.675	2.897	116.3	−440.413679
HPF^+	$^1A''$	2.754	2.901	116.6	−440.339354
PF_2^+	$^1A_1$		2.860	101.6	−539.422552
PF_2^+	$^3B_1$		2.876	116.5	−539.288625
PF_2^+	$^1B_1$		2.923	119.7	−539.172818

constraint of remaining orthogonal to the bond orbitals.

The bond orbitals of PF^+ in both the $^2\pi$ and $^4\Sigma^-$ states (shown in Figure 3) suggest a strongly ionic bond, since both bonds have significant F $2p_\sigma$ character. Also the nodal structure of these bonding orbitals is consistent with the fluorine $2p_\sigma$ orbital interacting with a phosphorus $3p_\sigma$ in the $^2\pi$ state and a phosphorus lobe in the $^4\Sigma^-$ state. Note also that while the singlet coupled lobes on PF^+ in the $^2\pi$ state are still localized essentially on phosphorus there is a noticeable fluorine contribution. Finally, we see from the contour map of the doubly occupied π_x orbital corresponding to the F $2p_\pi$ pair evidence that there is appreciable electron donation from F to P via the π system.

The Triatomics PH_2^+, PHF^+, and PF_2^+

A. GVB Calculations. We now imagine PH_2^+ being formed from PH^+ in the $^2\pi$ state by addition of a hydrogen atom. This hydrogen can bond to the singly occupied p orbital forming a $^1A_1$ state or it may bond to one of the lobe orbitals. If it bonds to a lobe orbital the resulting singly occupied lobe may couple its spin to either a singlet or triplet with the singly occupied p orbital giving rise to either a $^1B_1$ or $^3B_1$ state. From the results of the

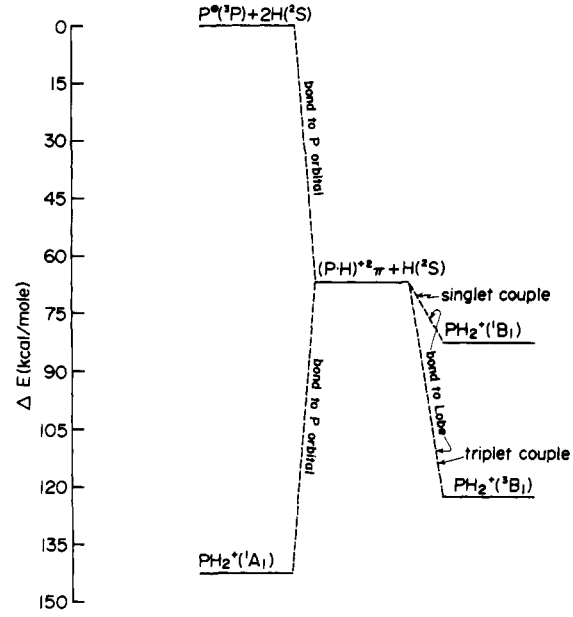

Figure 4. Schematic representation of the formation from the separated atoms of PH_2^+ in the $^1A_1$, $^3B_1$, and $^1B_1$ states.

PH^+ calculations we anticipate a clear preference for the interaction with a p orbital and expect the states of PH_2^+ will be in the order $^1A_1 < {}^3B_1 < {}^1B_1$. The results of detailed calculation presented in Figure 4 confirm this scenario as do the plots of the valence orbitals of the $^1A_1$ and $^3B_1$ states shown in Figure 5. Note also that the optimized geometries reported in Table III are consistent with what one would predict from these qualitative notions. Most remarkable is the similarity between the bond

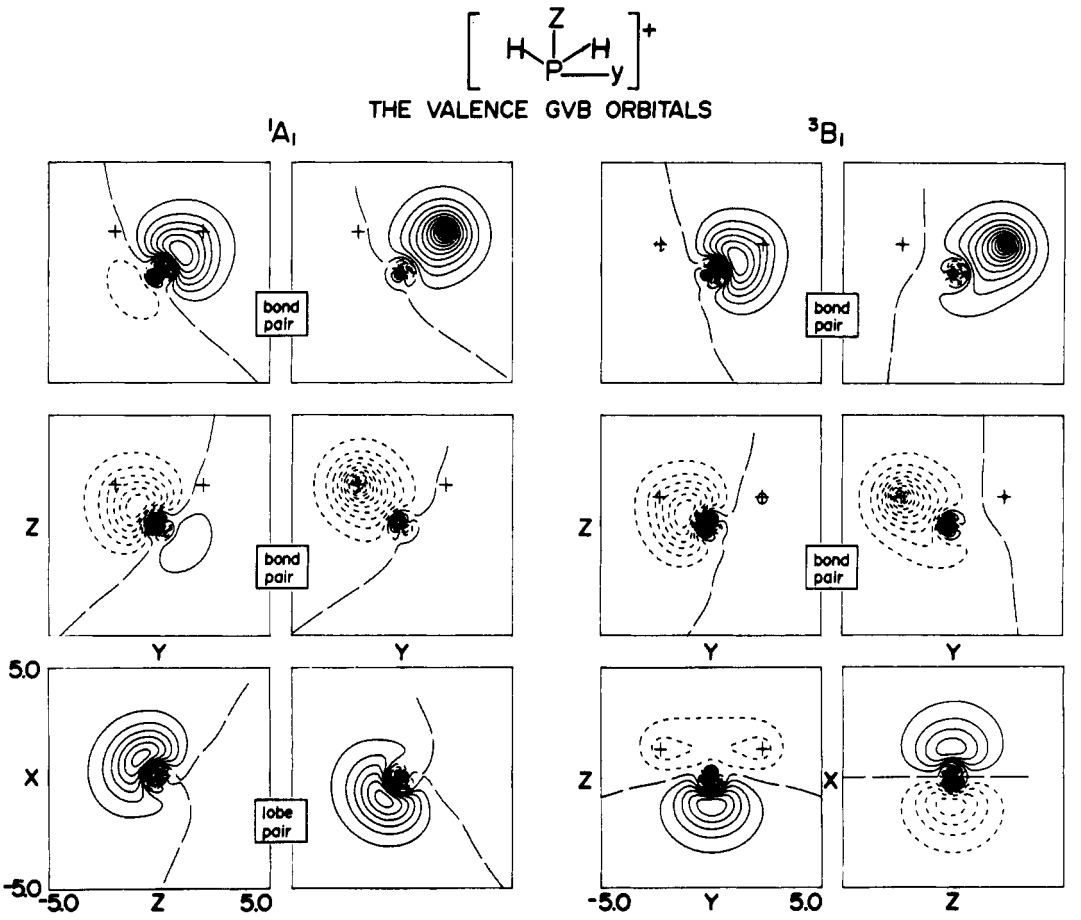

Figure 5. The GVB valence orbitals for PH_2^+ in the $^1A_1$, $^3B_1$, and $^1B_1$ states.

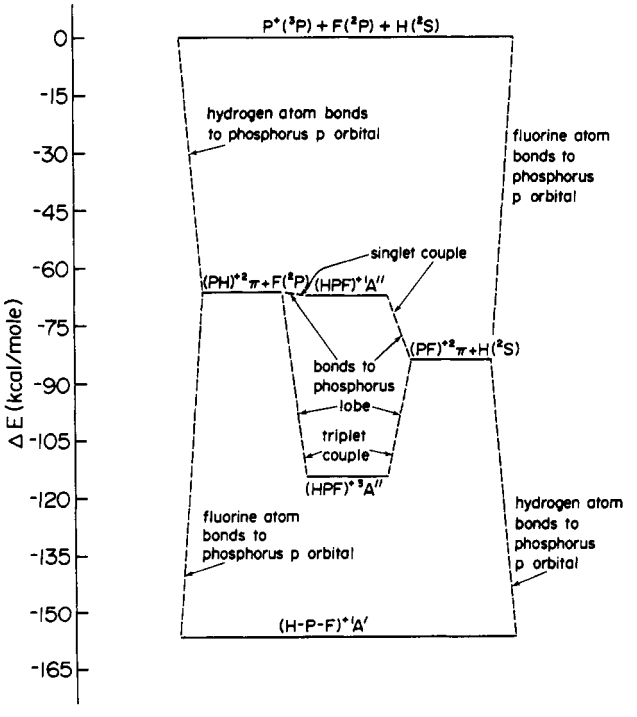

Figure 6. Schematic representation of the formation, from the separated atoms, of HPF^+ in the $^1A'$, $^3A''$, and $^1A''$ states.

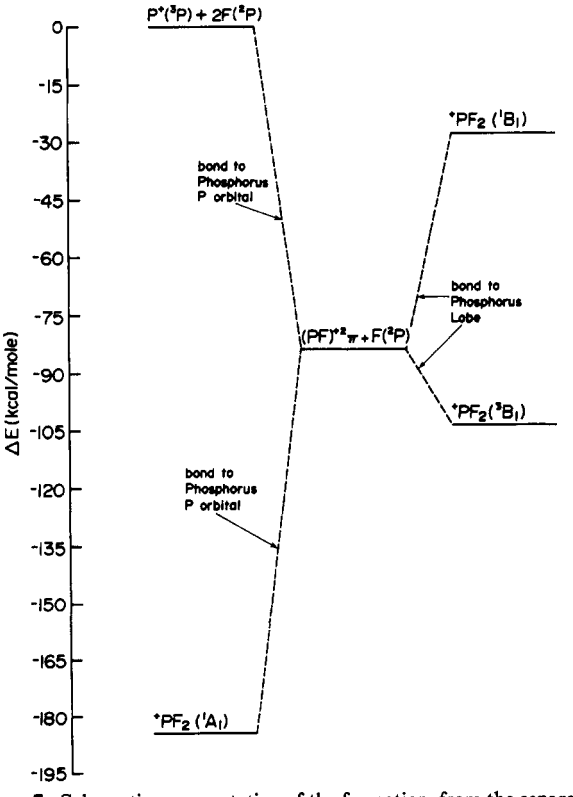

Figure 7. Schematic representation of the formation, from the separated atoms, of PF_2^+ in the $^1A_1$, $^3B_1$, and $^1B_1$ states.

orbitals in the $^1A_1$ state of PH_2^+ and those of the $^2\pi$ state of PH^+. Not only does the $^1A_1$ state of PH_2^+ have an angle of 94°, close to the idealized 90° suggested by the model just discussed, but the B_1 states have larger angles consistent with the hydrogen atom bonding to a "bent back lobe" in the $^2\pi$ state of PH^+. Of course both bonds are equivalent in PH_2^+ and when we imagine bonding first to a p orbital and then to a lobe we are idealizing the interaction significantly. The calculations do allow for the self-

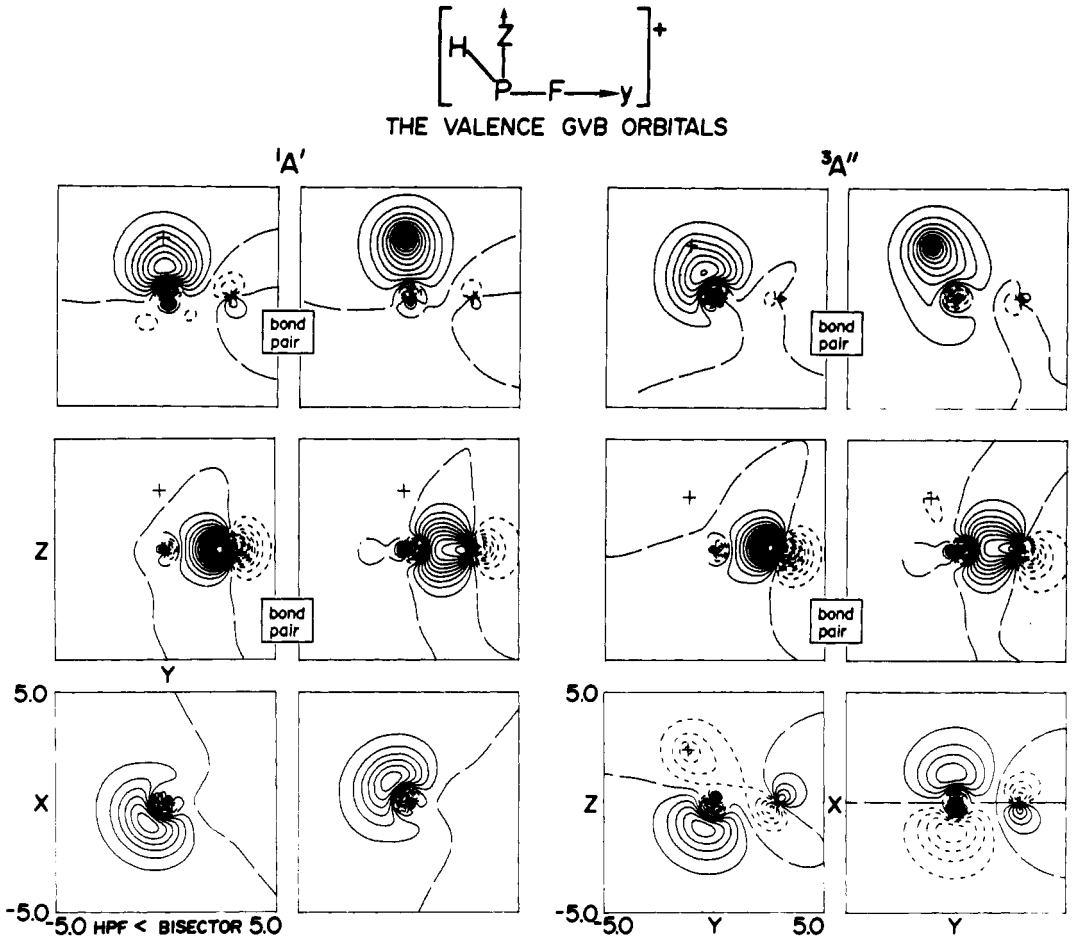

Figure 8. The GVB valence orbitals for HPF^+ in the $^1A'$ and $^3A''$ states.

Table IV. Electron Population and Charge Distribution in the Lowest Singlet and Triplet States of PH_2^+, HPF^+, and PF_2^+

	phosphorus						hydrogen			fluorine					
molecule	core	3s	$3p_\sigma$	$3p_\pi$	3d	Q	1s	2p	Q	core	2s	$2p_\sigma$	$2p_\pi$	3d	Q
$PH_2^+(^1A_1)$	10	1.71	2.17	0.06	0.11	+0.95	0.94	0.03	+0.03						
$PHF^+(^1A')$	10	1.75	1.59	0.14	0.16	+1.36	0.95	0.03	+0.02	2	1.91	3.47	1.94	0.05	−0.37
$PF_2^+(^1A_1)$	10	1.78	1.05	0.26	0.25	+1.66				2	1.91	3.53	1.84	0.05	−0.33
$PH_2^+(^3B_1)$	10	1.46	1.67	0.99	0.09	+0.79	0.86	0.03	+0.11						
$PHF^+(^3A'')$	10	1.41	1.20	1.03	0.17	+1.20	0.83	0.03	+0.14	2	1.91	3.45	1.93	0.05	−0.34
$PF_2^+(^3B_1)$	10	1.24	0.87	1.06	0.24	+1.59				2	1.91	3.39	1.94	0.05	−0.29

consistent adjustment of all the orbitals in the molecule and the subsequent bond orbitals in the B_1 states of PH_2^+ are intermediate in character between the PH^+ bonds in the $^2\pi$ and $^4\Sigma^-$ states as can be seen from Figures 2 and 5.

In a similar way we may imagine the formation of HPF^+ from PH^+ and F with the F bonding to a p orbital, forming the $^1A'$ state, or to a lobe (the $^3A''$ and $^1A''$ states) or the formation of PF_2^+ from PF^+ and F with F bonding to a p orbital (the $^1A_1$ state) or to a lobe (the $^1B_1$ and $^3B_1$ states). The results of our detailed calculations support the anticipated preference for bonding to a p orbital in that the closed shell singlet is the ground state of both molecules. The results for HPF^+ and PF_2^+ are schematically represented in Figures 6 and 7 and presented in detail in Table II. The contour maps of the GVB orbitals for the lowest singlet and triplet states of these molecules are shown in Figures 8 and 9. As with PH_2^+ and PH^+ the similarity between the P–H and P–F bonds in the $^2\pi$ states of PH^+ and PF^+ and the singlet states of HPF^+ and PF_2^+ is striking. One can also recognize the mixed $^2\pi$, $^4\Sigma^-$ character in the PH and PF bonds of the triplet states.

The results of the GVB calculations for the three molecules are summarized in Figure 10.

B. Charge Distribution. The results of a Mulliken population analysis[14] for the lowest singlet and triplet states of PH_2^+, HPF^+, and PF_2^+ are given in Table IV. In what follows the population of the 3s orbital is defined to be the total s population on P minus the 4s electrons associated with the core. Several features warrant comment. The uniformly higher and essentially constant 3s occupation of phosphorus in the singlet states is consistent with the view that the phosphorus uses essentially two p orbitals to bond to the ligands in these states. The lower and highly variable occupation of this orbital in the triplet states is consistent with the phosphorus using more 3s in its bonding orbitals (a mixture of p and lobe). When fluorine makes its electron demand on P both 3s and 3p electrons respond.

The increased occupancy of the $3p_\pi$ orbital on P in the singlet states as one goes from PH_2^+ to PF_2^+ is a direct measure of the back-donation to p from the F p_π orbitals which is crucial in the differential stabilization of the singlet relative to the triplet upon fluorine substitution.

The difference between the singlet and triplet charge distribution in each molecule is easily understood by noting that the triplet is formally obtained from the singlet by removing an electron from a lobe orbital and putting it into a π orbital. Since the π orbital

(14) R. S. Mulliken, *J. Chem. Phys.*, **23**, 1833 (1955).

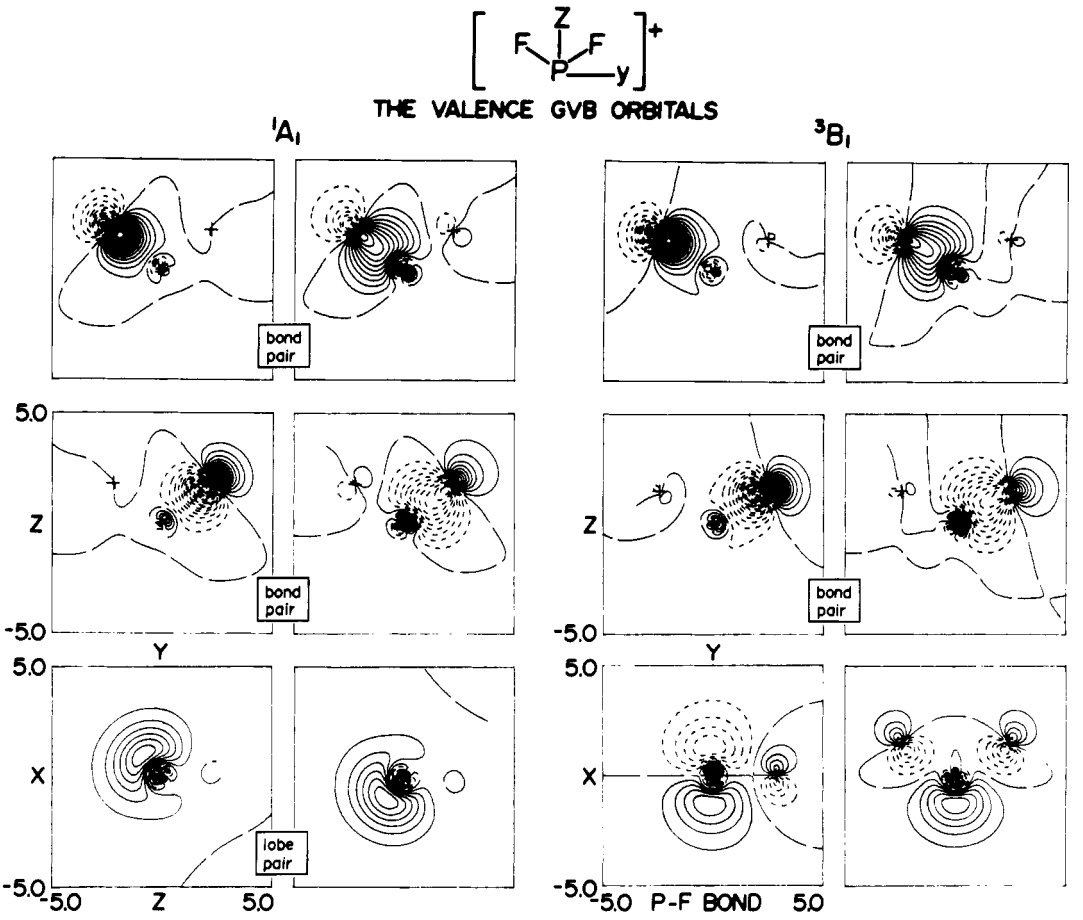

Figure 9. The GVB valence orbitals for PF_2^+ in the $^1A_1$ and $^3B_1$ states.

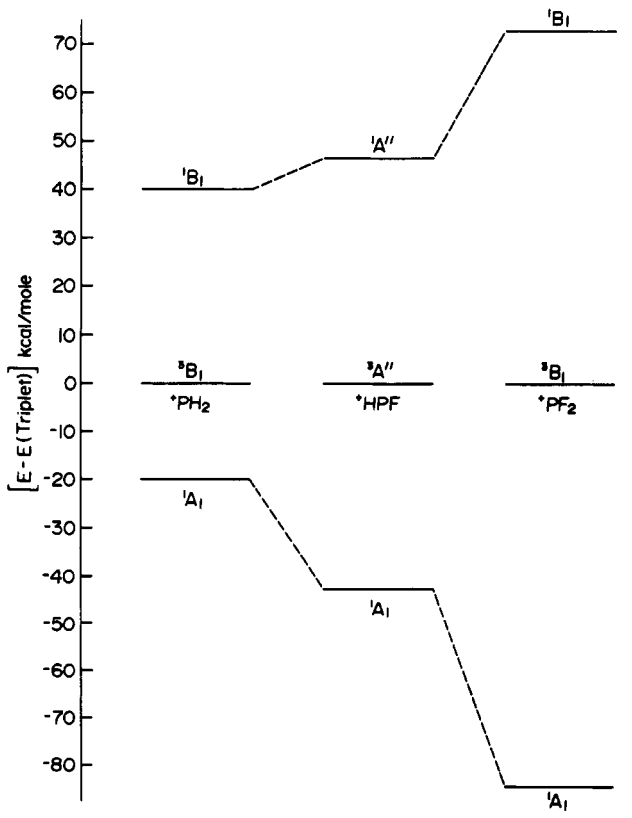

Figure 10. A GVB prediction for the relative energies of the first three electronic states of PH_2^+, HPF^+, and PF_2^+.

is more localized on P than the lobe this transfer invariably results in P gaining electrons and therefore hosting a less positive charge.

It is interesting to note that in $^+PH_2$ the positive charge is essentially on the P atom while in the isovalent nitrenium[15] ion NH_2^+ the positive charge is essentially on the hydrogen atoms. This very fundamental difference is a direct consequence of the relative electronegativity of P and N and should result in basic differences in the chemistries of the phosphenium and nitrenium ions. The shift in the charge on phosphorus upon fluoride substitution is in accord with our intuition.

C. CI Calculations on PH_2^+. In the GVB calculations discussed in the previous sections we correlated each bond in every molecule with two natural orbitals and, in addition, for the closed shell singlet states we split the lone pair with two natural orbitals. Consequently we anticipate that the major correlation effects have been accounted for and expect the singlet–triplet separation to be very realistic. As a check, and to quantify "very realistic", we have carried out CI calculations on the $^1A_1$, $^3B_1$, and $^1B_1$ states of the PH_2^+ molecule. The orbitals for the CI calculation were taken as the GVB orbitals of the equilibrium geometry of each state. These orbitals were divided into an occupied and a virtual set and two levels of CI were carried out. The first level was the GVB–CI in which all excitations within the GVB occupied set were allowed. The second level was a selected GVB + 1 + 2CI. In this technique one constructs all configurations which arise when no more than two electrons are permitted to be out of the occupied GVB space and in the virtual space. One then selects a subset of configurations using a cumulative procedure[16] so that the error resulting from using the selected list should be no more than 0.5×10^{-3} hartree or 0.3 kcal/mol.

The results are summarized in Table V and Figure 11 and show that the GVB description favored the $^1A_1$ state over the $^3B_1$ state by 4.3 kcal/mol. This suggests that the reported S–T separations

(15) J. F. Harrison and C. W. Eakers, *J. Am. Chem. Soc.*, **95**, 3467 (1973).
(16) R. C. Raffenetti, K. Hsu, and I. Shavitt, *Theor. Chim. Acta*, **45**, 33 (1977).

Table V. Configuration Interaction Results for PH_2^+

state	geometry		GVB	GVB/CI		GVB/CI + 1 + 2(selected)	
	R, bohr	θ, deg	energy, au	spin eigenfunctions	energy, au	spin eigenfunctions	energy, au
$^1A_1$	2.714	94.0	−341.56217	12	−371.56218	1327	−341.63804
$^3B_1$	2.667	121.5	−341.52969	10	−341.53129	2615	−341.61239
$^1B_1$	2.679	126.6	−341.46620	8	−341.47135	1908	−341.56026

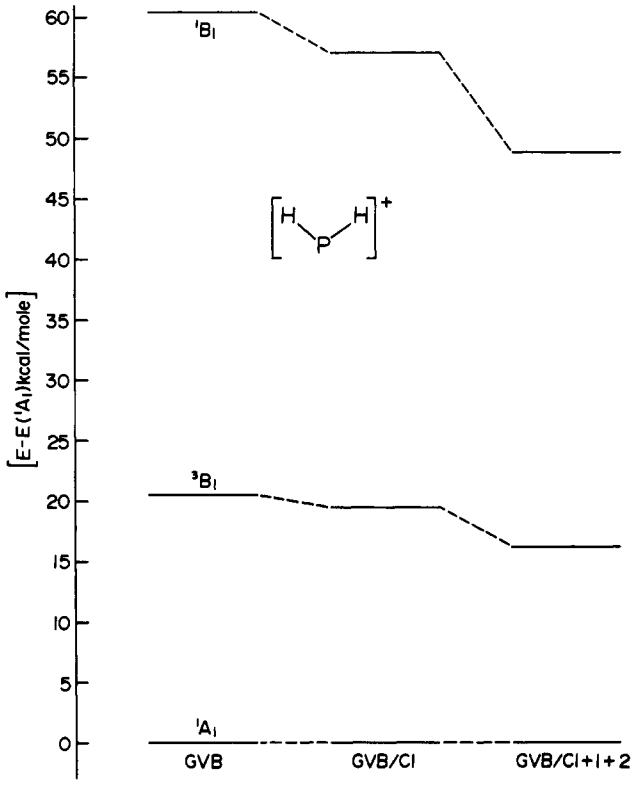

Figure 11. A comparison of the GVB and CI results for the $^1A_1$, $^3B_1$, and $^1B_1$ states of PH_2^+.

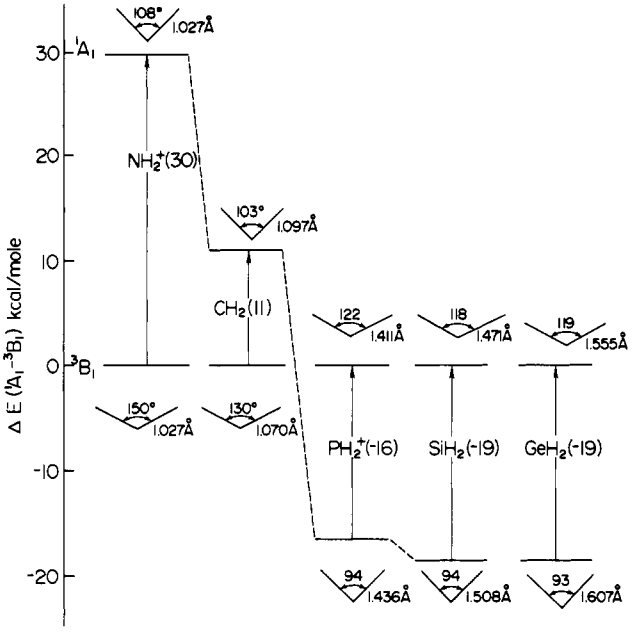

Figure 12. Theoretical triplet–singlet separation and geometry in the sequence $^+NH_2$, CH_2, $^+PH_2$, SiH_2, and GeH_2.

reported in Table III may be in error by a comparable amount. Most surprising is the change in the $^1A_1 - {}^1B_1$ separation from 60.2 kcal/mol (GVB) to 48.8 kcal/mol (selected CI) or a shift of approximately 0.5 eV. This suggests that our calculated singlet–singlet transition energies for HPF^+ and PF_2^+ may be too high by as much as 0.5 eV.

Previous Work and the Singlet–Triplet Separation in Related Molecules

The only previous ab-initio calculation on a phosphenium ion that we are aware of is the unpublished work by Cowley and McKee on $(NH_2)_2P^+$ which was cited in ref 4. We infer from their discussion that only the singlet state was investigated.

Our calculated singlet–triplet separation completes the important isovalent sequence CH_2, SiH_2, NH_2^+, and PH_2^+ and a comparison of the theoretical separations[7,17] in this sequence is given to the nearest kilocalorie/mole in Figure 12. Also included is the pseudopotential study of Barthelat[18] et al. on GeH_2 for completeness and the geometries of the various states. The first thing we note is that only NH_2^+ and CH_2 are triplets. Also, while there is a large difference in their singlet–triplet separations those of the remaining three molecules are very similar, reflecting the more gradual change in properties associated with atoms beyond the first row. While the separations in PH_2^+, SiH_2, and GeH_2 are sufficiently close that more refined calculations might alter the relative order, there is little doubt that all three have singlet ground states well below the first excited triplet.

Acknowledgment. The author wishes to thank Professor Joel Liebman for several informative discussions of phosphenium ion chemistry. The hospitality and advice of the theoretical chemistry group at the Argonne National Laboratory, in particular that of B. Botch, L. Harding, and T. Dunning, Jr., is gratefully acknowledged.

(17) S. D. Peyerimhoff and R. J. Buenker, *Chem. Phys.*, **42**, 167 (1979).
(18) Jean-Claude Barthelat, Bruno Saint Roch, George Trinquier, and Jacques Satgè, *J. Am. Chem. Soc.*, **102**, 4080 (1980).